Anexo A

Cálculo analítico de las propiedades de transmisión de las FSS

Marcuvitz [14] resuelve el problema de superficies infinitas formadas por franjas metálicas sin espesor. Siendo p la periodicidad del patrón, w el grosor del metal, g el grosor de los huecos, λ la longitud de onda, ϕ el ángulo de incidencia del campo $\vec{E}$ y θ el ángulo de incidencia del campo $\vec{H}$ sobre el FSS se obtiene las siguientes ecuaciones para el cálculo de los diferentes elementos pasivos que componen el modelo circuital de los FSS:

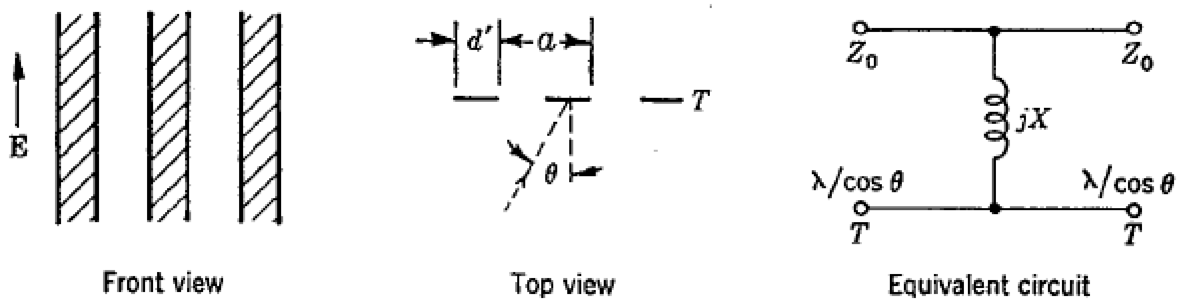

Figura A.1: Esquema de la superficie

$$F(p,w,\lambda,\phi) = j\frac{p\cos\phi}{\lambda}\left[\ln\left(\csc\left(\frac{\pi w}{2p}\right)\right) + G(p,w,\lambda,\phi)\right] \tag{A.1}$$

$$G(p,w,\lambda,\phi)=\frac{0.5\left(1-\beta^2\right)^2\left[\left(1-\frac{\beta^2}{4}\right)(C_++C_-)+4\beta^2C_+C_-\right]}{\left(1-\frac{\beta^2}{4}\right)+\beta^2\left(1+\frac{\beta^2}{2}-\frac{\beta^4}{8}\right)(C_++C_-)+2\beta^6C_+C_-} \tag{A.2}$$

$$C_\pm=\frac{1}{\sqrt{1\pm\frac{2p\sin\phi}{\lambda}-\left(\frac{p\cos\phi}{\lambda}\right)^2}}-1 \tag{A.3}$$

$$\beta=\sin\left(\frac{\pi w}{2p}\right) \tag{A.4}$$

A partir de estas ecuaciones, se obtiene el parámetro S_{21}. Para el caso de una FSS sin vidrio nos encontramos ante un circuito como el de la figura A.2. X_L se corresponde con la impedancia resultante a partir de las ecuaciones de Marcuvitz y que se explican en el capítulo 2.

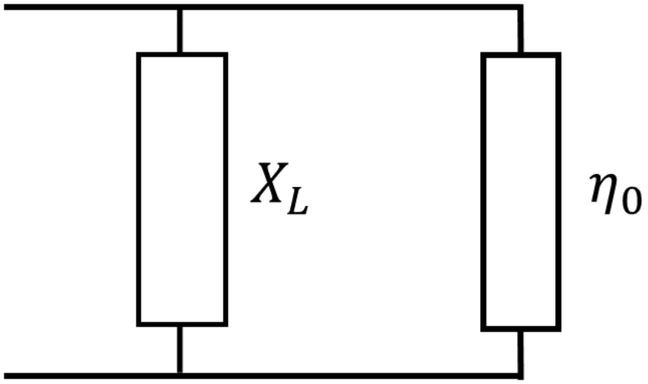

Figura A.2: Circuito equivalente sin vidrio

Por lo tanto se obtiene la impedancia de entrada del circuito calculando la suma de ambas impedancias en paralelo:

$$Z_{in}=\frac{X_L\times\eta_0}{X_L+\eta_0} \tag{A.5}$$

Por otro lado, en el caso de que haya vidrio, se añade una línea de transmisión de longitud igual al espesor del dieléctrico por lo que no nos vale con calcular la impedancia en paralelo con la impedancia característica, sino que hay que calcular primero la impedancia equivalente tal y como se muestra en la ecuación A.6.

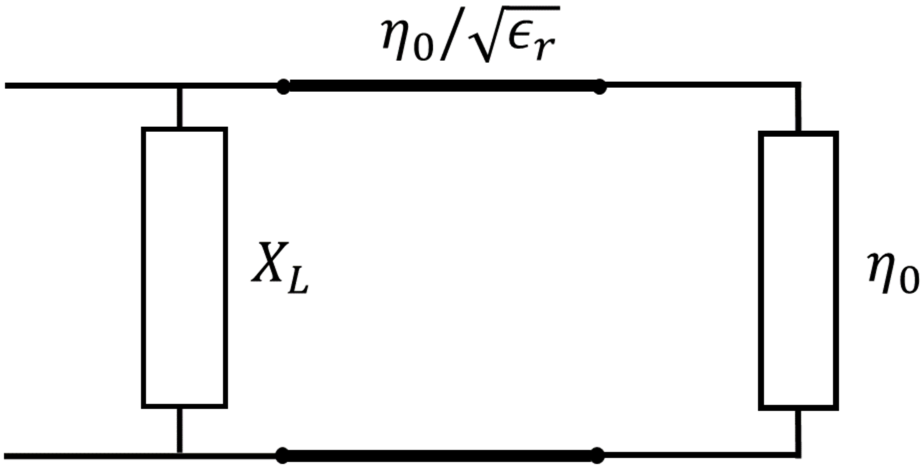

Figura A.3: Circuito equivalente con vidrio

$$Z_0 = \frac{\eta_0}{\sqrt{\epsilon_r}} \frac{1 + j\tan\frac{\beta l}{\sqrt{\epsilon_r}}}{\frac{1}{\sqrt{\epsilon_r}+j\tan\beta l}} \tag{A.6}$$

$$Z_{in} = \frac{X_L \times Z_0}{X_L + Z_0} \tag{A.7}$$

Una vez calculada la impedancia de entrada se puede calcular el coeficiente de transmisión con la ecuación siguiente:

$$S_{21} = \frac{2Z_{in}}{Z_{in} + \eta_0} \tag{A.8}$$

Los diferentes tipos de patrones explicados en el capítulo 3 pueden calcularse siguiendo estos pasos con el siguiente código de Matlab:

```
%% Paso alto
clear all; close all;
palto = textread('Palto27-6.txt')
```

```
palto = reshape(palto,46,4);
f = 0.5e9:0.1e9:5e9;
lambda = 3e8./f;
epsr = 2.1;
w = 6e-3;
p = 27e-3;
eta0 = 277;
betal = (2*pi*4e-3)./(lambda/sqrt(epsr));
Zi = eta0/sqrt(epsr)*(1+j*tan(betal)/sqrt(epsr))./(1/sqrt(epsr)+j*tan(
    betal));

X_L = eta0*fun(p,w,lambda);
Zin = (Zi.*X_L)./(X_L+Zi);
S11 = (Zin-eta0)./(Zin+eta0);
S11 = abs(S11).^2;
S21 = 1 - S11;
figure, plot(f,10*log10(S11)); hold on
plot(f,10*log10(abs(S21)));
plot(f,palto(:,3));
plot(f,palto(:,4));
xlabel('Frecuencia (Hz)'); ylabel('Magnitud (dB)');
legend('S_1_1 teo','S_2_1 teo','S_1_1 sim', 'S_2_1 sim');

%% Paso bajo
clear all; close all;
pbajo = textread('Pbajo27-6.txt');
pbajo = reshape(pbajo,46,4);
f = 0.5e9:0.1e9:5e9;
lambda = 3e8./f;
```

```
epsr = 2.1;
g = 6e-3;
p = 27e-3;
eta0 = 277;
betal = (2*pi*4e-3)./(lambda/sqrt(epsr));
Zi = eta0/sqrt(epsr)*(1+j*tan(betal)/sqrt(epsr))./(1/sqrt(epsr)+j*tan(betal));

B_C = 4*epsr*fun(p,g,lambda);
X_C = eta0./B_C;

Zin = (X_C.*Zi)./(X_C+Zi);
S11 = (Zin-eta0)./(Zin+eta0);
S21 = (2*Zin)./(Zin + eta0);
figure, plot(f,20*log10(abs(S11))); hold on
plot(f,20*log10(abs(S21)));
plot(f,pbajo(:,3));
plot(f,pbajo(:,4));
xlabel('Frecuencia (Hz)'); ylabel('Magnitud (dB)');
legend('S_1_1 teo','S_2_1 teo','S_1_1 sim', 'S_2_1 sim');


%% Paso banda
clear all; close all;
f = 0.5e9:0.1e9:5e9;
pbanda = textread('Pbanda50-40-12.txt');
pbanda = reshape(pbanda,46,4);
lambda = 3e8./f;
epsr = 2.1;
```

```
g = 3e-3;
d = 50e-3;
p = 60e-3;
eta0 = 120*pi;
betal = (2*pi*4e-3)./(lambda/sqrt(epsr));
Zi = eta0/sqrt(epsr)*(1+j*tan(betal)/sqrt(epsr))./(1/sqrt(epsr)+j*tan(
    betal));

F_c= fun(p,g,lambda);
B_c = 2*epsr*d/p*F_c;
X_c = eta0./B_c;

F_l2 = fun(p,p-d,lambda);
X_l2 = eta0*F_l2;

ZZ = X_c;
Zin = X_l2.*ZZ./(X_l2+ZZ);
Zin = Zin.*Zi./(Zin+Zi);
S11 = (Zin - eta0)./(Zin + eta0);
S11 = abs(S11).^2;
S21 = 1 - S11;

figure,
plot(f,20*log10(abs(S11))); hold on;
plot(f,20*log10(abs(S21)));
plot(f,pbanda(:,3));
plot(f,pbanda(:,4));
xlabel('Frecuencia (Hz)'); ylabel('Magnitud (dB)');
legend('S_1_1 teo','S_2_1 teo','S_1_1 sim', 'S_2_1 sim');
```

```

%% Elimina banda
clear all; close all;
ebanda = textread('Ebanda50-40-12.txt');
ebanda = reshape(ebanda,46,4);
f = 0.5e9:0.1e9:5e9;
lambda = 3e8./f;
epsr = 2.1;
w = 12e-3;
d = 40e-3;
p = 60e-3;
eta0 = 120*pi;
betal = (2*pi*4e-3)./(lambda/sqrt(epsr));
Zi = eta0/sqrt(epsr)*(1+j*tan(betal)/sqrt(epsr))./(1/sqrt(epsr)+j*tan(
    betal));

F_c= fun(p,p-d,lambda);
B_c = 4*epsr*w/p*F_c;
X_c = eta0./B_c;

F_l = fun(p,w,lambda);
X_l = eta0*(d)/p*F_l;

Zin = X_l+X_c;
Zin = Zin.*Zi./(Zin+Zi);
S11 = (Zin - eta0)./(Zin + eta0);
S11 = abs(S11).^2;
S21 = 1 - S11;

```

```
figure,
plot(f,10*log10(abs(S11))); hold on;
plot(f,10*log10(abs(S21)));
plot(f,ebanda(:,3));
plot(f,ebanda(:,4));
xlabel('Frecuencia (Hz)'); ylabel('Magnitud (dB)');
legend('S_1_1 teo','S_2_1 teo','S_1_1 sim','S_2_1 sim');


%% Funcion
function F = fun(p,w,lambda)
beta = sin(pi/2*w/p);
beta2 = beta^2;
C = 1./sqrt(1-(p./lambda).^2)-1;
G_num = 0.5*(1-beta2)^2*((1-beta2/4)*2*C+4*beta2*C.^2);
G_den = (1-beta2/4)+beta2*(1+beta2/2-(beta2^2)/8)*2*C+2*(beta^6)*C.^2;
G = G_num./G_den;
F = j*p./lambda.*(log(csc(pi/2*w/p))+G);
end
```

Anexo B

Características de las antenas utilizadas

- Model: XDJ-800/2500DS-9
- Frequency Range-MHz: 824-960/1710-2500
- Band Width-MHz: 136/790
- Gain-dBi: 9
- Horizontal Beam Width:45
- Vertical Beam Width:30
- VSWR: ≤ 1.5
- Input Impedance-Ω:50
- Polarization:Vertical
- Maximum Input Power-W: 50
- Connector: N
- Mechanical Specifications
- Antenna Size-mm :290*200*60
- Weight-kg:0.5
- Color:White.

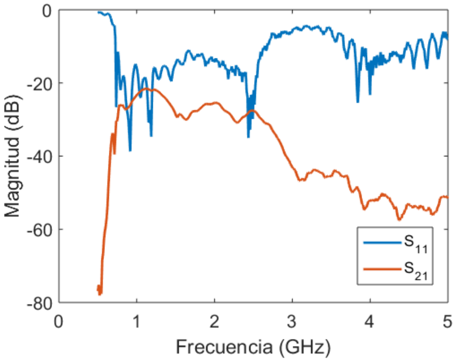

X0019OFD8B

Ultra Wide band UWB...IVALDI TAPERED SLOT
New

TSA600

Ultra-Wideband PCB Tapered Slot Antenna

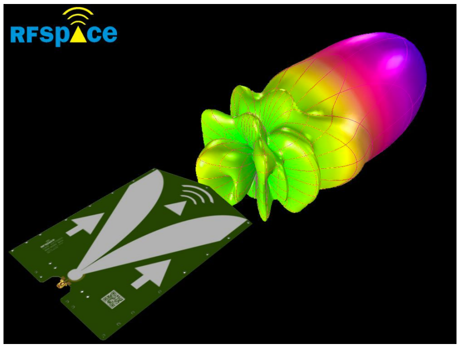

Features:

- High Performance, broad frequency range of 600 MHz to 6 GHz+
- Linear polarized with excellent gain over entire range
- Low VSWR over full range with no resonances
- Clean impulse response
- Very low loss substrate
- Individually calibrated and tested
- Low cost
- SMA output connector
- Adjustable polarization
- 25 Watt CW

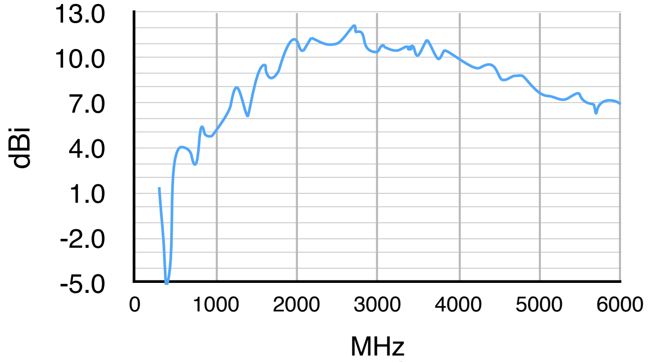

Antenna Gain

Applications:

- Ground Penetrating Radars (GPR)
- Radio communications LTE,WIMAX,WIFI,PCS,UWB,GSM,HDTV,IoT
- Signals and communications Intelligence (SIGINT, COMINT, ELINT)
- Pulse Radar
- Broadband Software Defined Radio (SDR) Antenna
- EMC testing
- Spectrum analysis
- Direction finding

Description:

The RFSPACE TSA600 is a high performance, low cost, wideband antenna optimized for high gain, low VSWR and broadband response. The matching network has been optimized for best VSWR and a clean impulse response. Every TSA600 antenna is individually tuned and tested. The TSA600 is ideal as a wideband transmit or receive antenna for today's wireless communications.

Specifications:

Gain:	11 dBi @ 2.4 GHz
	10 dBi @ 4.0 GHz
	7 dBi @ 6.0 GHz

VSWR: 600 MHz - 6000 MHz <2.0:1 Typical.
Power Handling: 25 Watts
Aperture width: 240 mm
Length: 330 mm
Weight: 0.5 lbs
Connector: 50Ω SMA edge mount
MSPR: $69 Qty 1-5
$62 Qty 5+

* Specifications subject to change without notice.

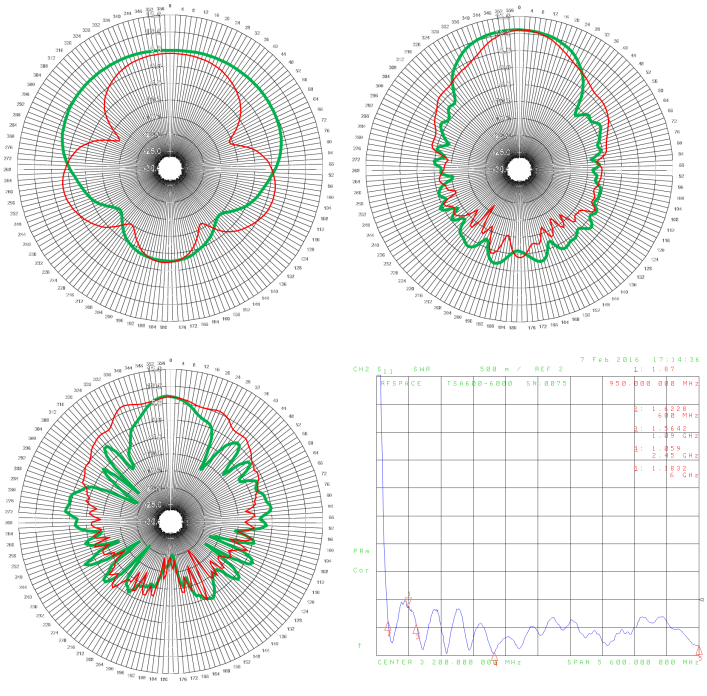

Antenna patterns at 600 MHz, 2400 MHz and 6000 MHz + VSWR

Rev. 04/01/2017 © 2015 RFSPACE, INC.

http:// www.rfspace.com
Twitter: @rfspace
antennas tested at: http://antennatestlab.com

RFSPACE

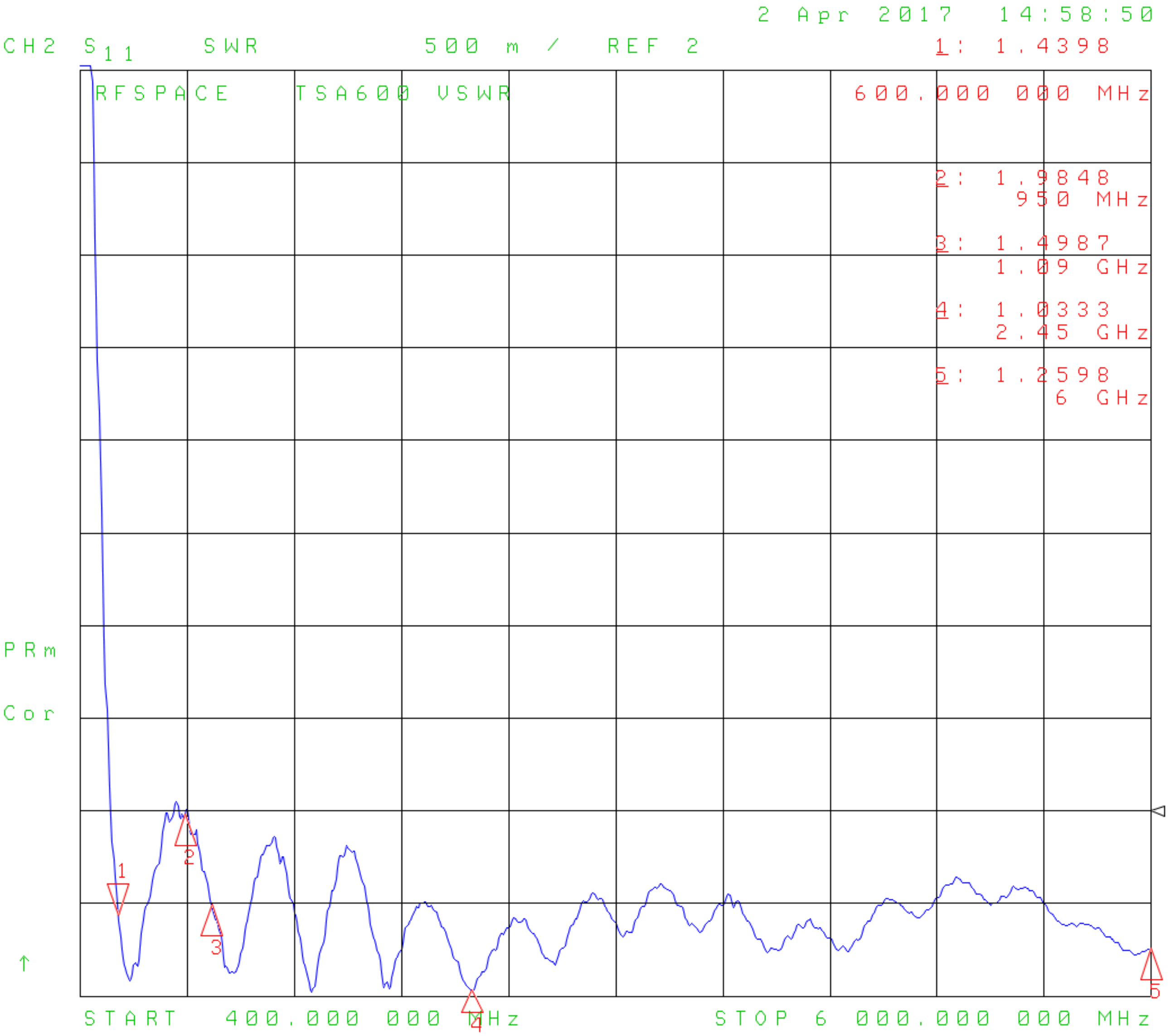

Typical Antenna VSWR Plot

Available from:

amazon.com HAM RADIO OUTLET universal radio inc. ebay

Rev. 04/01/2017 © 2015 RFSPACE, INC.

http:// www.rfspace.com
Twitter: @rfspace
antennas tested at: http://antennatestlab.com

RFSPACE

Bibliografía

[1] *Ariplak Low E-SP. Capas de Altas Prestaciones*. Ariño Duglass.

[2] *Ariplak Solar. Capas de control solar*. Ariño Duglass.

[3] Luc Burnier et al. "Energy saving glazing with a wide band-pass FSS allowing mobile communication: upscaling and characterisation". In: *IET Microwaves, Antennas and Propagation* 11.10 (2017), pp. 1449–1455.

[4] Antonio L.P.S. Campos et al. "Software for project and analysis of Frequency Selective Surfaces". In: *Microwaves, Optoelectronics and Electromagnetic Applications* 11.1 (June 2012), pp. 56–67.

[5] Filipo Costa, Agostino Monorchio, and Giuliano Manara. "An overview of equivalent circuit modeling techniques of frequency selective surfaces and metasurfaces". In: *ACES journal* 29.12 (Diciembre 2014), pp. 960–976.

[6] G. H. Dadashzadeh, M. H. Amini, and A. R. Mallahzadeh. "Equivalent circuit model for square ring slot frequency selective surface". In: *Journal of communication engineering* 3.1 (2014), pp. 23–32.

[7] Institute of electrical and Inc. electronics Engineers. *IEEE Standard method for measuring the effectiveness of Electromagnetic Shielding Enclosures*. IEEE. Diciembre 1997.

[8] Mahmoud Fallah, Alireza Ghayekhloo, and Ali Abdolali. "Design of frequency selective band stop shield using analytical method". In: *Microwaves, Optoelectronics and Electromagnetic Applications* 14.2 (Diciembre 2015), pp. 217–228.

[9] David Ferreira et al. “Square loop and slot frequency selective surfaces study for equivalent circuit model optimization”. In: *IEEE transactions on antennas and propagation* 63.9 (Sept. 2015), pp. 3949–3955.

[10] *Frequency selective surface, complementary split. Ring Resonator.* COMSOL Multiphysics.

[11] Paul Harms, Raj Mittra, and Wai Ko. “Implementation of the Periodic Boundary Condition in the Finite-Difference Time-Domain Algorithm for FSS structures”. In: *IEEE Transactions on Antennas and Propagation* 42.9 (Sept. 1994), pp. 1317–1323.

[12] Benjamin Hooberman. *Everything you ever wanted to know about Frequency-Selective surface filters but were afraid to ask.* May 2005.

[13] Ghaffer I. Kiani et al. *Transmission improvement of useful signals through energy saving glass windows using frequency selective surfaces.* Tech. rep. Macquarie University and University of Lund, 2008.

[14] Nathan Marcuvitz. *Waveguide Handbook.* Institution of Electrical Engineers, London: Peter Peregrinus Ltd., 1951.

[15] Cristian Morari and Ionut Blan. *Methods for determining shielding effectiveness of materials.* Tech. rep. INCDIE ICPE-CA.

[16] Ben A. Munk. *Frequency Selective Surfaces. Theory and design.* New York: John Wiley and sons, Inc., 2000.

[17] Irfan Ullah et al. *Transmission Improvement of UMTS and Wi-Fi Signals Through Energy Saving Glass Using FSS.* Tech. rep. Edith Cowan University, 2011.

[18] Isabel Vela Pérez. *Desarrollo de capas transparentes con propiedades eléctricas sobre vidrio plano mediante pulverización catódica de ITO.* Sept. 2015.

[19] Björn Widenberg and José Víctor Rodríguez Rodríguez. *Design of Energy Saving Windows with High Transmission at 900 MHz and 1800 MHz.* Tech. rep. Lund University, Enero 2002.